

## Simultaneous Determination of Chemical Diffusion and Surface Exchange Coefficients of Oxygen by the Potential Step Technique

Stefan Diethelm,<sup>a</sup> Alexandre Closset,<sup>a</sup> Kemal Nisançioğlu,<sup>a,c,\*</sup> Jan Vanherle,<sup>a</sup>  
A. J. McEvoy,<sup>a,\*</sup> and Turgut M. Gür<sup>b</sup>

<sup>a</sup>Laboratoire de Photonique et Interfaces, École Polytechnique Fédérale de Lausanne, CH 1015 Lausanne, Switzerland

<sup>b</sup>Center for Materials Research, Stanford University, Stanford, California 94305-4045, USA

Oxygen diffusion is treated in a dense electronically conducting cobaltate pellet blocked ionically on one surface, electronically on the other, and sealed on its cylindrical periphery. A procedure is developed for extracting the chemical diffusion and surface exchange coefficients for oxygen by use of the asymptotic equations derived for the current response to a potential step at short and long times. It is shown that, while the formation of interfacial phases by reaction between the sample and the electrolyte may affect the surface exchange coefficient, the chemical diffusion coefficient data determined by the present approach are independent of such interfacial phenomena. The consistency of data obtained from several specimens with varying thickness and manner of interfacing with the electrolyte validates the diffusion model and the method used for data analysis. An oxygen permeation cell is also developed in this work as a modification of the diffusion cell. The new cell allows monitoring of the permeation rate by electrochemical means. The steady-state permeation data obtained by the permeation cell are consistent with the chemical-diffusion and surface-exchange coefficients measured by the blocked diffusion cell as long as the assumptions of the related theoretical models are satisfied. This is a further validation of the diffusion model and the related methodology developed here for obtaining the necessary data for characterizing oxygen exchange and transport in such materials.

© 1999 The Electrochemical Society. S0013-4651(98)06-048-0. All rights reserved.

Manuscript submitted June 11, 1998; revised manuscript received December 10, 1998.

Relaxation techniques are commonly used for the evaluation of the chemical diffusion coefficient of oxygen in electronically conducting perovskites, considered for applications as cathodes in solid oxide fuel cells and membranes for the separation of oxygen from gas mixtures at high temperatures.<sup>1-7</sup> These techniques involve the measurement of time variation of weight or conductivity of the specimen, or the flux of the diffusing species in response to a rapid change in the surrounding oxygen activity. Diffusion coefficients are obtained by fitting the relaxation data to the theoretical solution of Fick's second law, expressed in various forms depending on the relaxation experiment. The accuracy and reliability of the diffusion coefficients obtained depend on the methods of analysis used in fitting the relaxation data to the theoretical equations, as well as on the specimen quality.<sup>5</sup>

Among the relaxation techniques, electrochemical methods are of particular interest, because they allow easy and accurate determination of oxygen activity and flux by measurement of potential and current, respectively. In particular, the solid-state electrochemical technique and cell design proposed by Belzner et al.<sup>1</sup> provide the advantages of monitoring the oxygen activity at the specimen surface by potential measurement with respect to a reference electrode and the oxygen flux by measuring the ionic current due to one-dimensional lattice diffusion of oxygen through the specimen. Furthermore, the technique is suitable for the measurement of a large amount of data as a function of temperature and oxygen activity in a relatively short period from a single specimen. Since the diffusion test in addition yields coulometric titration data, information about the nonstoichiometry of the sample can also be obtained. The technique has successfully been applied for studying oxygen diffusion and nonstoichiometry in manganates.<sup>2</sup>

However, when applied to the study of cobaltates, difficulties were reported in the interpretation of data by using the solutions of Fick's first law for one-dimensional lattice diffusion, although limitation on mass transfer by surface exchange of oxygen was taken into account.<sup>5</sup> It was concluded that the oxygen transport in these materials occurred through high diffusivity paths, while the relaxation data were controlled by intragrain diffusion and exchange reaction at the grain boundaries.

<sup>c</sup> Permanent address: Department of Electrochemistry, Norwegian University of Science and Technology, N-7034 Trondheim, Norway.

\* Electrochemical Society Active Member.

The importance of considering surface-exchange limitations in connection with diffusion processes in solids has been pointed out by several authors<sup>5-8</sup> and various kinetic models have been invoked for the observed relaxation processes. The most commonly used model,<sup>5-9</sup> which is known as the linear rate law, assumes that the surface exchange reaction obeys first-order kinetics. The advantage of the latter in comparison with more complicated models<sup>10</sup> is the convenience provided in the analysis of experimental relaxation data by use of analytical solutions of the diffusion equations. Several approaches are used in the analysis of relaxation data, such as direct fits to the complete solution of Fick's law by nonlinear regression,<sup>8</sup> or fits to particular solutions with lattice diffusion or surface exchange dominating,<sup>5,8</sup> and more recently, complex plane analysis of Fourier transformed data by use of equivalent circuit analogs.<sup>6,7</sup>

In this paper, we investigate further the alternative of using simple asymptotic expressions for short and long time response for the analysis of relaxation data obtained in the presence of surface exchange limitations, with suggestions to check the consistency of calculated parameters. Certain modifications are introduced to the cell design proposed by Belzner et al. in order to overcome the experimental problems associated with the study of cobaltates.

The materials selected for the study are highly defective cobaltates  $\text{SrCo}_{0.5}\text{Fe}_{0.5}\text{O}_{3-\delta}$ <sup>4,5,11</sup> and  $\text{SrFeCo}_{0.5}\text{O}_x$ .<sup>3,12</sup> However, the present study, rather than dwelling on the material properties, focuses on the validity of the theoretical model for diffusion of oxygen in such oxides and the proposed methodology for data analysis.

### Experimental

**Cell design and construction.**—One of the electrochemical cell designs used in this study, the classical "blocked cell" proposed by Belzner et al.,<sup>1</sup> is shown in Fig. 1a. It consisted of a specimen pellet blocked electronically by an ionically conducting electrolyte slab on one surface. The opposite surface was blocked ionically by a platinum foil. The cylindrical surface of the pellet was coated with gold and further sealed with glass, as described in earlier work,<sup>1,5</sup> to prevent direct oxygen ingress from ambient air. The gold layer prevent ed direct contact between the sample and the glass seal.

A YSZ slab was used as the electrolyte. A thin layer of porous platinum was added between the pellet and the YSZ as a spacer to avoid undesired reaction between the components of the pellet and the zirconia.<sup>5</sup> The platinum was also presumed to act as a catalyst for the interfacial transport of oxygen. As alternative electrolytes, yttria-

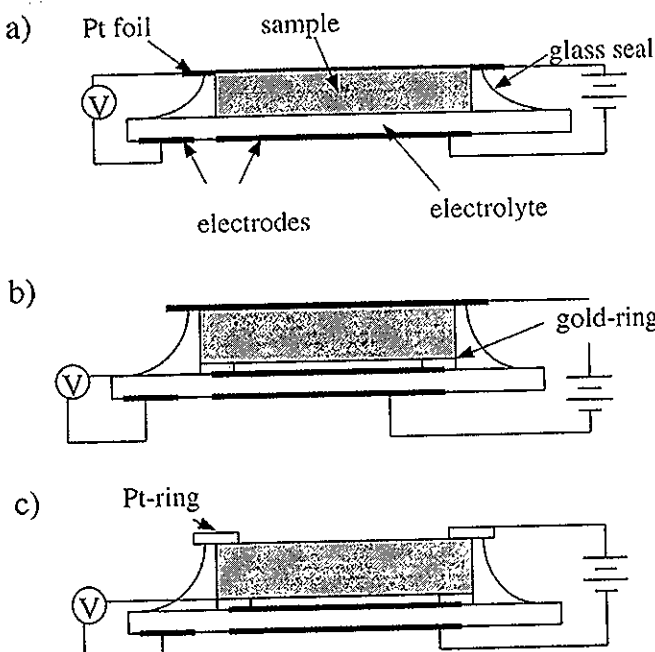


Figure 1. Cell designs used for the potential step measurements: (a) blocked cell, (b) blocked cell with a gold ring spacer, (c) open cell with a gold ring spacer.

and gadolinia-doped ceria, known to be less reactive to cobaltates, were also used without the porous Pt spacer. The opposite face of the electrolyte was coated with a thin layer of porous platinum in two separate patches to act as the air counter electrode and the reference electrode, as shown in the figure.

Figure 1b shows a variation of the previous design. Instead of having the electrolyte in direct contact with the cobaltate specimen, a gold ring (50  $\mu\text{m}$  thick) was added as a spacer. The upper surface of the electrolyte inside the gas spacer was again coated with a thin layer of porous Pt, such that the electrolyte acted as an oxygen pump.

The third variant, the "open cell design," was similar to the previous cells except that the top surface of pellet was exposed to ambient air, with only a thin platinum ring on top acting as the current collector. All cells were clamped between two alumina (or quartz) tubes at the center of a cylindrical furnace.

Because of the thermal expansion mismatch between the constituents of the cell, thermocycling had to be avoided in order to prevent cracking of the sample. Thus, the cells were heated up to the temperature of measurement (800–975°C) only once. The cells, once cooled back to room temperature, were not used again. This implies that special care was required in the assembly of the cell to reach a satisfactory seal quality once the cell was heated.

**Materials.**—The  $\text{SrCo}_{0.5}\text{Fe}_{0.5}\text{O}_{3-\delta}$  powder was available from earlier work,<sup>4,5</sup> and  $\text{SrFeCo}_{0.5}\text{O}_x$  powder was provided by Norsk Hydro a.s. The powders were compressed into 6 mm diam pellets, and the two compounds were sintered for 8 h at 1200 and 1180°C, respectively. Both surfaces of the sintered pellets were metallographically polished through 1  $\mu\text{m}$  diamond spray. The density of  $\text{SrCo}_{0.5}\text{Fe}_{0.5}\text{O}_{3-\delta}$  specimens was  $90 \pm 1\%$  of the theoretical value. Owing to the uncertainty regarding structure, no theoretical density data are available for  $\text{SrFeCo}_{0.5}\text{O}_x$ . However, the absolute densities of the specimens were measured as  $4.8 \pm 0.2 \text{ g/cm}^3$ .

The YSZ slabs were obtained by compression of  $\text{Y}_2\text{O}_3\text{-ZrO}_2$  (8 mol %) powder (Tosoh) into 15 to 20 mm diam pellets, which were sintered for 4 h at 1450°C. Both surfaces were metallographically polished as above. The densities obtained were  $98 \pm 1\%$  of the theoretical value. The gadolinia- and yttria-doped ceria (GdDC and YDC) electrolyte slabs were prepared from Gd- and Y-doped ceria

powders, respectively, also available from earlier work.<sup>13</sup> The sintering and polishing procedure was the same as for the YSZ slabs. The thickness of electrolyte slabs used in the cells were in the range 0.7 to 1.3 mm.

### Theory

Since the specimens are good electronic conductors, the potential gradient across the pellet is negligible. A potential step applied to the specimen relative to the reference electrode by use of a potentiostat is thus equivalent to a step in the oxygen activity at the electrolyte-specimen interface under the conditions that the charge-transfer reaction at the pellet-electrolyte interface is fast, and ionic transport through the electrolyte is not rate limiting. As a response to this abrupt change in the interfacial oxygen activity, the concentration of oxygen in the specimen will relax through chemical diffusion of oxygen to a new equilibrium distribution fixed by the applied potential. The resulting time-dependent flux of oxygen across the electrolyte-specimen interface manifests itself as an ionic current which is monitored as a function of time. For the cell designs discussed, a one-dimensional diffusion process is a reasonable assumption.

In view of the foregoing assumptions, it is possible to express the transient diffusion of oxygen by Fick's second law

$$\frac{\partial C}{\partial t} = \frac{\partial}{\partial x} \left( \tilde{D} \frac{\partial C}{\partial x} \right) \quad [1]$$

where  $\tilde{D}$  is the chemical diffusion coefficient and  $C$  is the concentration of the diffusing species expressed in  $\text{mol/cm}^3$ .<sup>14,15</sup> For  $\text{SrCo}_{0.5}\text{Fe}_{0.5}\text{O}_{3-\delta}$ , the diffusing species is believed to be oxygen vacancies, whereas for  $\text{SrFeCo}_{0.5}\text{O}_x$ , it is interstitial oxygen according to Ref. 12. The coefficient  $\tilde{D}$  is related to the ionic diffusion coefficient  $D_i$  (which obeys the Nernst-Einstein equation) by<sup>14</sup>

$$\tilde{D} = \left( \frac{\partial \ln a^*}{\partial \ln C^*} \right) D_i = W D_i \quad [2]$$

where  $W$  ( $= \partial \ln a^* / \partial \ln C^*$ ) is the so-called enhancement factor. The parameters  $a^*$  and  $C^*$  refer to the activity and the concentration of the neutral species, respectively. Equation 2 indicates that  $\tilde{D}$  can be a strong function of concentration. However, for small changes in the nonstoichiometry,  $\tilde{D}$  can be considered as independent of concentration.

**Blocked cell design.**—For the designs depicted in Fig. 1a and b, the boundary conditions required for solving Eq. 1 are similar, i.e., the flux of the ionic species is blocked on the top surface ( $x = 0$ ) and is prescribed on the bottom surface ( $x = L$ , where  $L$  is the thickness of the pellet) by a rate equation corresponding to the surface exchange reaction. If the latter obeys first-order kinetics, then the condition at  $x = L$  can be expressed as

$$\tilde{D} \left( \frac{\partial C}{\partial x} \right) = k(C_{\text{eq}} - C) \quad [3]$$

where  $k$  is the rate constant and  $C_{\text{eq}}$  is the equilibrium concentration to which the concentration of diffusing species within the solid will tend at infinite time.

From the general solution to Eq. 1 satisfying the prescribed boundary conditions, it is possible to derive for the measured current the expression<sup>16</sup>

$$I(t) = Q \sum_{n=1}^{\infty} \frac{2\Lambda^2 \tilde{D} \exp(-\lambda_n^2 \tilde{D} t / L^2)}{L^2 (\lambda_n^2 + \Lambda^2 + \Lambda)} \quad [4]$$

where  $Q$  is the total charge passed as  $t$  tends to infinity,  $\lambda_n$  are the positive roots of

$$\lambda_n \tan \lambda_n = \Lambda \quad [5]$$

and  $\Lambda = kL/\tilde{D}$ .

In its infinite series form, Eq. 4 is not convenient for routine data analysis, especially at short times. It is thus desirable to obtain

approximations for asymptotic cases. The solution to Eq. 4 at small times can be expressed in the form<sup>17</sup>

$$I(t) = \frac{Qk}{L} \exp\left(\frac{k^2 t}{\tilde{D}}\right) \operatorname{erfc}\left(k\sqrt{\frac{t}{\tilde{D}}}\right) \quad t \ll L/k \quad [6]$$

Equation 6 can still be reduced to a simpler form by series expansion of the complementary error function to obtain

$$I(t) = \frac{Qk}{L} \left(1 - 2k\sqrt{\frac{t}{\pi\tilde{D}}}\right) + O(t) \quad t \ll \tilde{D}/k^2 \quad [7]$$

As  $Q$  can be obtained by integrating the current with respect to time,  $k$  and  $\tilde{D}$  can separately be found by plotting  $I(t)$  vs.  $t^{1/2}$ . The parameter  $k$  can be evaluated from the intercept of this plot at  $t = 0$ , and  $\tilde{D}$  from the slope.

At long times, Eq. 4 reduces to the form

$$I(t) = \frac{2Qk^2}{\tilde{D}(\lambda_1^2 + \Lambda^2 + \Lambda)} \exp\left(\frac{-\lambda_1^2 \tilde{D}t}{L^2}\right) \quad t \gg L^2/\tilde{D}\pi^2 \quad [8]$$

The intercept and slope of  $\ln I$ - $t$  plots give an independent possibility of extracting the parameters  $k$  and  $\tilde{D}$  values from the experimental relaxation data.

The data for the blocked cell design in addition yields coulometric titration data since the change in the oxygen concentration  $\Delta C$  resulting from a negative potential step is directly related to the corresponding charge  $\Delta Q$  extracted from the specimen. Assuming that the specimen volume  $V$  does not change significantly during the process, we can write the expression

$$\Delta C = -\frac{\Delta Q}{2VF} \quad [9]$$

where  $F$  is Faraday's constant. For small amplitude potential steps, i.e., small changes in nonstoichiometry, the slope of the coulometric titration curve ( $dE/dC$ ) can be approximated by

$$\frac{dE}{dC} \cong \frac{\Delta E}{\Delta C} = -\frac{2FV\Delta E}{\Delta Q} \quad [10]$$

which in turn is related to the enhancement factor according to the expression<sup>18</sup>

$$W = -\frac{2FC^* dE}{RT dC} \quad [11]$$

where  $R$  is the ideal gas constant. Thus, estimation of the enhancement factor from coulometric titration data requires the knowledge of the concentration of neutral lattice oxygen in the specimen.

*Open cell design.*—For the open cell design, the irreversible boundary condition expressed by Eq. 3 has to be considered at both surfaces of the pellet. In this paper we are concerned with the use of this cell at steady state and close to equilibrium condition, i.e., for small steady-state currents. The steady-state current resulting from a difference of oxygen activity, attained by applying a potential difference  $V$  across the electrolyte in Fig. 1a, is given by<sup>16</sup>

$$I_{ss} = \frac{2FS\Delta C_{eq}}{1/k_0 + 1/k_L + L/\tilde{D}} = K\Delta C_{eq} \quad [12]$$

where  $S$  is the pellet area perpendicular to the direction of diffusion,  $\Delta C_{eq}$  ( $= C_0 - C_L$ ) is the difference in the equilibrium concentration of diffusing species corresponding to the conditions at  $x = 0$  and  $x = L$ , and  $k_0$  and  $k_L$  are the exchange rate constants at the two respective surfaces. The "polarization resistance" of the cell can be expressed as

$$R_p = \lim_{I_{ss} \rightarrow 0} \frac{dV}{dI_{ss}} = \frac{dE}{dC^*} \lim_{I_{ss} \rightarrow 0} \frac{dC^*}{dI_{ss}} \quad [13]$$

By combining with Eq. 11 and 12, and since  $dC^* = -dC$ , we obtain

$$R_p = \frac{RTW}{2FC^*K} \quad [14]$$

The linear polarization data obtained by use of the open-cell design is of interest for comparison to the parameters extracted from the blocked cell data and, thereby, for checking the consistency of the results, as is shown in the remainder of the paper.

## Results

*Blocked cell.*—The seal quality of the cells was checked by applying a potential across the diffusion cell, equivalent to a lowering of the oxygen partial pressure at the pellet-electrolyte interface. After equilibrium was attained, i.e., the cell current decayed to zero, the circuit was switched open, and the open-circuit potential was monitored as a function of time. The ability of the cell to maintain that potential within 1 mV over a period of 1 h was taken to indicate a well-sealed cell. However, in some cases, especially when ceria electrolyte was used, a leakage current was present, and it had to be corrected for as described in the related earlier work.<sup>5</sup> In this special case, the leakage current was due to the electronic conductivity of the electrolyte. At 850°C, an electronic leakage current of  $\sim 40 \mu\text{A}$  was typically observed at an applied potential of  $-20 \text{ mV}$  vs. air. This corresponds to an electronic conductivity of  $\sim 7 \cdot 10^{-4} \text{ S/cm}$ , in agreement with the available data for GdDC.<sup>19</sup>

The long time and short time responses of the blocked cell design with a gold ring spacer to a  $-20 \text{ mV}$  potential step are shown in Fig. 2 and 3, respectively. The long-time response displays a clear exponential decay behavior as expected from the asymptotic Eq. 8. For the short time response, the asymptotic behavior predicted by Eq. 7 is less evident although a linear section but is apparent when the current relaxation data are plotted vs.  $\sqrt{t}$ , as shown in Fig. 3. The time domain in which this linear fit is valid is determined by the constraint  $t \ll \tilde{D}/k^2$  at large times (Eq. 7), and the capacitive discharge of the oxygen in the gas space between the specimen and the electrolyte at short times, as will be justified later in the paper.

We selected the following approach, among several possible, in extracting the relevant parameters from the relaxation data

1. Obtain  $Q$  by integration of the  $I$ - $t$  data, corrected for the leakage current in the manner described earlier.<sup>5</sup>

2. Obtain  $k$  and the chemical diffusion coefficient from the intercept and slope of fitting the data to the asymptotic Eq. 7, as in Fig. 3. Let these values obtained from the short time analysis be denoted as  $k_s$  and  $\tilde{D}_s$ , respectively.

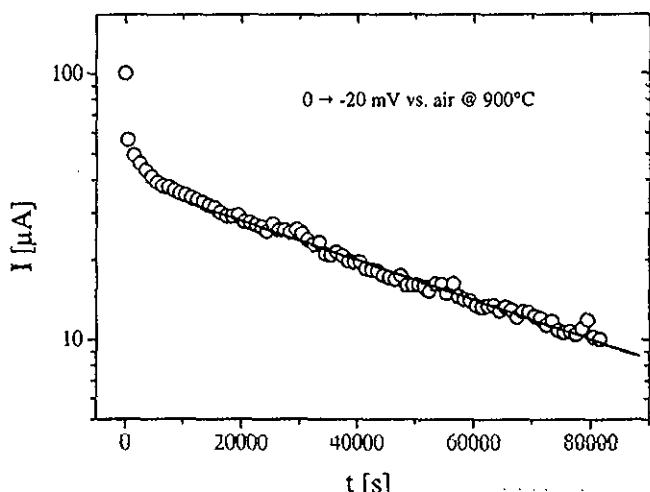


Figure 2. Current relaxation data corresponding to a potential step from 0 to  $-20 \text{ mV}$  vs. air for a pellet specimen of  $\text{SrFeCo}_{0.5}\text{O}_x$  with the gold ring design at 900°C. The straight line is a fit to Eq. 8 of the data collected at  $t > 10,000 \text{ s}$ .

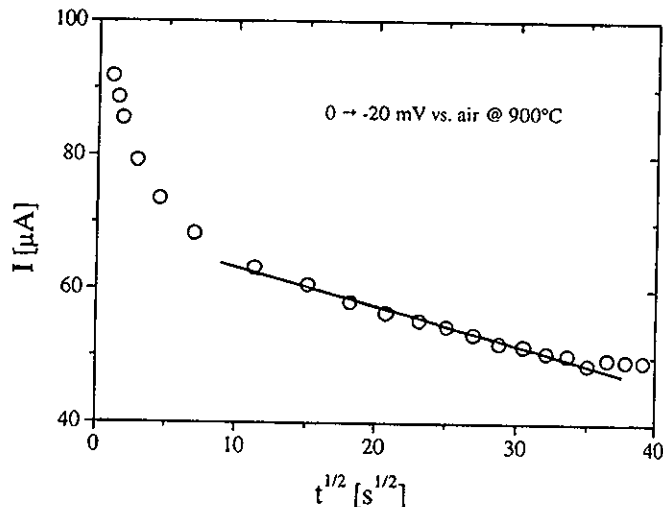


Figure 3. The data in Fig. 2 plotted vs.  $\sqrt{t}$ . The straight line is a fit to Eq. 7 of the data in the range 100 to 1250 s.

3. By using the  $k_s$ ,  $\tilde{D}_s$ , and  $Q$  values obtained as above, evaluate  $\Lambda$  and  $\lambda_1$  from Eq. 5, and calculate the chemical diffusion coefficient, this time from the slope of fitting the data to the asymptotic Eq. 8, as in Fig. 2. This value is denoted as  $\tilde{D}_\ell$ .

4. Calculate  $k$  from the pre-exponential factor of fitting the data to the asymptotic Eq. 8 using the  $\lambda_1$ ,  $\Lambda$ ,  $Q$ , and  $\tilde{D}_\ell$  values obtained above. This value is denoted as  $k_\ell$ .

5. Check if the time domains used for the asymptotic fits satisfy the ranges of validity for Eq. 7 and 8.

6. Fit the relaxation data to the general solution of Fick's second law, Eq. 4, by using the values  $k_s$ ,  $Q$ , and  $\tilde{D}_\ell$  as obtained above, for a final validity check. This is an arbitrary selection of parameters;  $k_\ell$  instead of  $k_s$  or  $\tilde{D}_s$  instead of  $\tilde{D}_\ell$  can just as well be used.

The chemical diffusion coefficients obtained from several electrochemical cells in this manner, using different cell designs, are summarized in Table I. The consistency between the two values of  $k$  and  $\tilde{D}$ , obtained separately, gives a first appreciation of the validity of the theoretical model and methodology used for data analysis.

As an example for the validity tests suggested above, we investigate whether the choice of time domains used for the asymptotic fits represented by Fig. 2 and 3 agree with the time constraints of Eq. 8 and 7, respectively. By using the data given on the figures and their captions, we calculate  $t \gg L^2/\tilde{D} \pi^2 \approx 3500$  s and  $t \ll \tilde{D}/k_2 \approx 15000$  s, respectively, for the two plots, and by inspection of fit domains in the figures, it can be seen that the necessary time constraints are obeyed.

As a further example of the validity checks performed, the relaxation data are compared with the  $I-t$  curve calculated by using the

first three terms of the general solution of Fick's second law, Eq. 4, and the  $\tilde{D}_\ell$  and  $k_s$  values extracted by the procedure outlined above. The result is shown in Fig. 4 by the dotted line, which is superimposed by the solid line along most of the time axis. The use of larger number of terms in the series did not improve the fit significantly. It can be concluded that there is an excellent agreement between the data and the general solution, except at very short times, where the relaxation behavior is controlled by the capacitive discharge of the gas pocket as indicated earlier. The solid line corresponds to the general solution corrected for this effect, as is discussed below.

The time constant of the short-time capacitive effect was investigated by replacing the cobaltate specimen in Fig. 1c by a YSZ slab (without the Pt ring current collector on top), thereby maintaining approximately the same volume of gas pocket as in the actual runs and, at the same time, eliminating the relaxation behavior related to the cobaltate sample. The gold ring spacer was used as the current collector in this experiment. Although not shown, the current response to an identical potential step as in the actual experiments exhibited a pure exponential decay with a time constant of about 2 s, i.e., the capacitive current became insignificant after about 50 s. This result provided an appropriate lower time limit for the short-time analysis.

Based on the foregoing, furthermore, the capacitive current could be expressed by the equation

$$I_c = \frac{Q_c}{\tau_c} e^{-t/\tau_c} \quad [15]$$

where the subscript c refers to the capacitive relaxation due to the gas pocket. This term was added to the right side of Eq. 4 as a correction term. The solid line in Fig. 4 corresponds to the fit by using this correction term.

Figure 5 depicts an Arrhenius plot for the chemical diffusion coefficients, based on the long-time analysis. It should be stressed that this plot compiles values obtained from different specimens of varying thickness and electrochemical cell designs (cf. Table I). Two different electrolytes are also used. The details about these design parameters are specified in the figure caption. Possible differences in the specimen quality, known to result from the fabrication process<sup>5,20</sup> have to be considered to explain part of the scatter, while the use of different electrolytes must be of minor importance in this respect. The activation energies obtained from the slopes of the Arrhenius plot are  $200 \pm 25$  and  $70 \pm 35$  kJ/mol for  $\text{SrCo}_{0.5}\text{Fe}_{0.5}\text{O}_{3-\delta}$  and  $\text{SrFeCo}_{0.5}\text{O}_x$ , respectively, in good agreement with the data reported earlier for the two compounds.<sup>4,3</sup>

The data in Fig. 5 correspond to specimens with varying thickness, as can be discerned from the figure caption. It is not possible to observe a specific thickness dependence of the diffusion coefficient from these data, contrary to earlier observations for  $\text{SrCo}_x\text{Fe}_{1-x}\text{O}_{3-\delta}$ .<sup>5</sup> The earlier results had also suggested independence of the relaxation time constant, obtained by the semilogarithmic

Table I. Chemical diffusion and surface exchange coefficients obtained by fitting the relaxation data to the asymptotic flux expressions: a, Blocked cell on YSZ with a gold ring spacer; b, blocked cell on ceria; c, blocked cell on YSZ.

Sample	Cell	$L$ (mm)	$T$ (°C)	$k_s$ (cm/s)	$k_\ell$ (cm/s)	$\tilde{D}_s$ (cm <sup>2</sup> /s)	$\tilde{D}_\ell$ (cm <sup>2</sup> /s)	$W/C^a$
$\text{SrFeCo}_{0.5}\text{O}_x$	a	2.742	800	$2.4 \cdot 10^{-6}$	$2.3 \cdot 10^{-6}$	$9.5 \cdot 10^{-7}$	$8.9 \cdot 10^{-7}$	2365
			900	$8.1 \cdot 10^{-6}$	$8.5 \cdot 10^{-6}$	$1.17 \cdot 10^{-6}$	$1.32 \cdot 10^{-6}$	5670
	b	1.085	900	$9.9 \cdot 10^{-6}$	$8.6 \cdot 10^{-6}$	$3.8 \cdot 10^{-6}$	$3.47 \cdot 10^{-6}$	945
	b	1.36	975	$1.9 \cdot 10^{-5}$	$9.8 \cdot 10^{-6}$	$4.1 \cdot 10^{-6}$	$2.34 \cdot 10^{-6}$	1120
	a	1.837	800	$7.6 \cdot 10^{-6}$	$5.3 \cdot 10^{-6}$	$1.5 \cdot 10^{-6}$	$1.1 \cdot 10^{-6}$	1220
			900	$1.3 \cdot 10^{-5}$	$1.3 \cdot 10^{-5}$	$2.1 \cdot 10^{-5}$	$2.2 \cdot 10^{-5}$	1571
$\text{SrCo}_{0.5}\text{Fe}_{0.5}\text{O}_{3-\delta}$	a	0.613	900	$6.4 \cdot 10^{-5}$	$6.3 \cdot 10^{-5}$	$1.6 \cdot 10^{-5}$	$1.5 \cdot 10^{-5}$	1153
	c	0.873	888	$3.6 \cdot 10^{-5}$	$4.6 \cdot 10^{-5}$	$1.36 \cdot 10^{-5}$	$1.4 \cdot 10^{-5}$	1037
	b	1.352	900	$3.5 \cdot 10^{-5}$	$3.1 \cdot 10^{-5}$	$2.5 \cdot 10^{-5}$	$2.1 \cdot 10^{-5}$	1462

<sup>a</sup> This work.

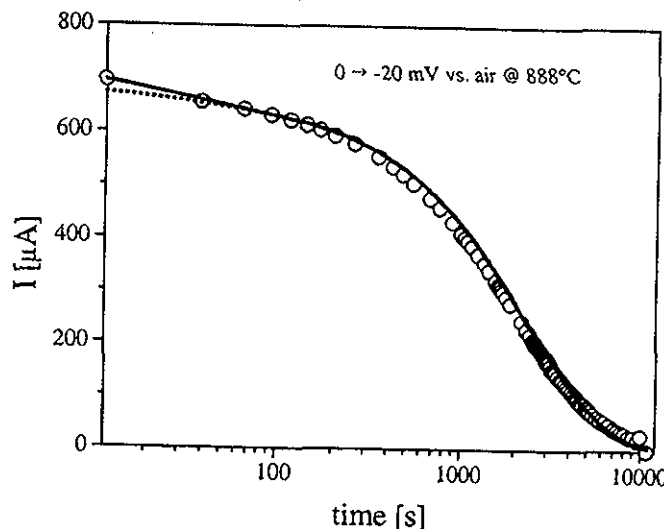


Figure 4. Current relaxation data corresponding to a potential step of  $-20$  mV vs. air for a  $\text{SrCo}_{0.5}\text{Fe}_{0.5}\text{O}_{3-\delta}$  blocked cell. The dashed line is a fit of complete data ( $0 < t < 10,000$  s) to the first three terms of Eq. 4. The solid line is a fit to the same expression with an additional exponential term for the capacitive response of the interfacial gas pocket.

mic fit of the long-time data, on the specimen thickness, suggesting the presence of high diffusivity paths combined with slow intragrain diffusion.<sup>5</sup> However, in this study, the relaxation time constant shows a clear thickness dependence at a given temperature, as shown in Fig. 6, also in disagreement with the earlier results, but as expected on our model.

The other important kinetic and thermodynamic parameters evaluated from the potential step data are reported also in Table I. The enhancement factor  $W$  for  $\text{SrCo}_{0.5}\text{Fe}_{0.5}\text{O}_{3-\delta}$  can be calculated from the  $W/C^*$  data as about 85 and 110 at 800 and 900°C, respectively, by assuming that  $\delta \ll 3$ . These values agree well with the previously reported data for the same compound by making the same assumption.<sup>4</sup> The exchange coefficient  $k$  is expected to depend on the particular conditions existing on the specimen surface adjacent to the electrolyte. However, such an effect is not apparent from the values

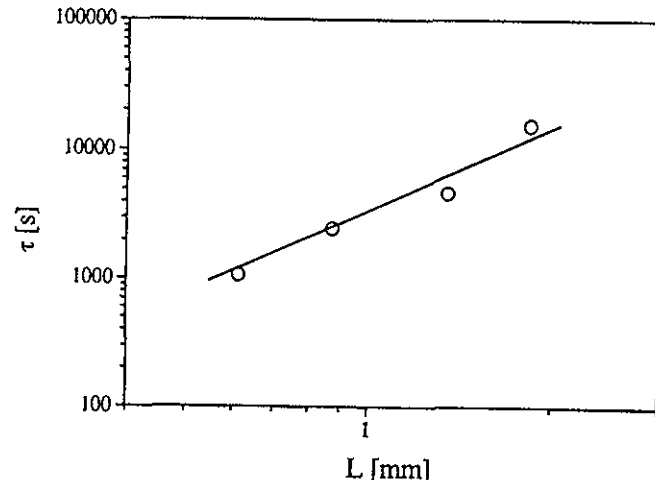


Figure 6. Thickness dependence of the relaxation time constant  $\tau$  for  $\text{SrCo}_{0.5}\text{Fe}_{0.5}\text{O}_{3-\delta}$  samples at 900°C.

for different types of cobaltate-electrolyte interfaces in Table I, within the scatter limits of the data.

*Open cell.*—Limited number of runs were performed with the open cell for the sole purpose of comparing the results with the data obtained from the blocked cell. The current response of an open cell to a potential step reaches a steady state value  $I_{ss}$  after a long transient. An analysis of the transient data is outside the present scope. The steady-state values corresponding to different applied potential steps are shown in Fig. 7. At small potentials ( $<20$  mV), a linear relation between the steady-state current and applied voltage can clearly be observed for  $\text{SrCo}_{0.5}\text{Fe}_{0.5}\text{O}_{3-\delta}$ , whereas a similar relationship is not evident for  $\text{SrFeCo}_{0.5}\text{O}_x$ . The nonstoichiometry of the compound  $\text{SrCo}_{0.5}\text{Fe}_{0.5}\text{O}_{3-\delta}$ , expressed in the form  $W/C^*$ , can thus be estimated from the slope of the linear part and Eq. 14, by using the  $k$  and  $\tilde{D}$  values obtained from the blocked cell data. If the same  $k$  value is assumed to apply at both surfaces of the specimen, the  $W/C^*$  value obtained in this manner is about 700, which is to be compared with the value of about 1000 obtained from the analysis of the blocked cell data for the same compound at the same temperature (888°C). A reasonable agreement is thus obtained for the  $W/C^*$  values determined by use of two different cell designs based on two dif-

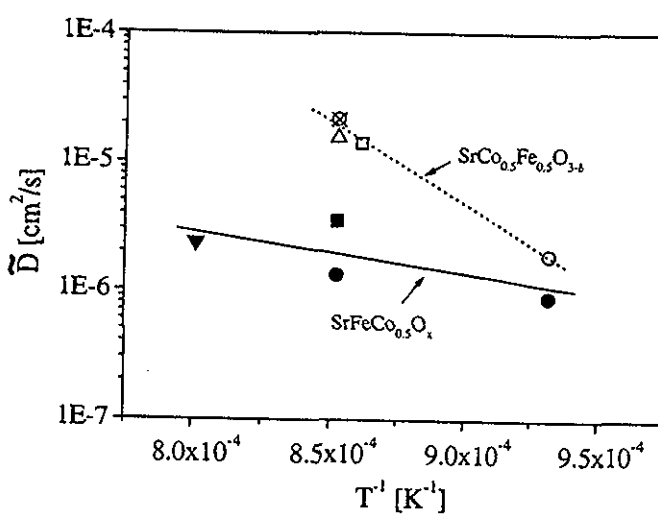


Figure 5. Arrhenius plot for diffusion coefficients calculated from current transients following potential steps of  $-20$  mV vs. air.  $\text{SrFeCo}_{0.5}\text{O}_x$  pellets separated from YSZ electrolyte with a gold ring spacer [ $L = 2.742$  mm (●)] and in direct contact with ceria electrolyte [ $L = 1.085$  mm (■),  $L = 1.36$  mm (▼)].  $\text{SrCo}_{0.5}\text{Fe}_{0.5}\text{O}_{3-\delta}$  pellets separated from YSZ electrolyte with a gold-ring spacer [ $L = 1.837$  mm (○),  $L = 0.613$  mm (Δ)] and in direct contact with YSZ [ $L = 0.873$  mm (□)] and ceria [ $L = 1.352$  mm (×)].

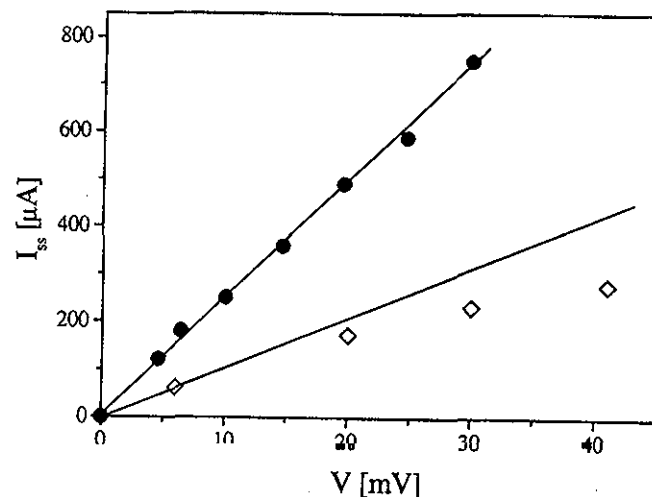


Figure 7. Steady-state polarization data obtained with the open cell for small applied potentials. (●)  $\text{SrCo}_{0.5}\text{Fe}_{0.5}\text{O}_{3-\delta}$  at 888°C ( $L = 0.873$  mm), (○)  $\text{SrFeCo}_{0.5}\text{O}_x$  at 850°C ( $L = 2.98$  mm). The straight lines are the tangents to the curves at  $I_{ss} = 0$ .

ferent modes of operation. A similar analysis performed for the compound  $\text{SrFeCo}_{0.5}\text{O}_x$  by using the slope of the tangent drawn to the origin of Fig. 7 gave a poor agreement with the data obtained from the blocked cell because the  $W/C^*$  obtained in this manner was about an order of magnitude lower than the values reported in Table I.

**Interfacial structures.**—The cross sections of two blocked electrochemical cells were investigated by optical and scanning electron microscopy (SEM). Close attention was given to the interfacial region between the cobaltate pellets and the electrolyte. For a  $\text{SrCo}_{0.5}\text{Fe}_{0.5}\text{O}_{3-\delta}$ -YSZ cell, which had previously been maintained at 850°C for more than six weeks, the cobaltate specimen exhibited a fragmented morphology close to the interface. Qualitative X-ray EDX analysis of the interface with a 15 kV beam, revealed the presence of the constituents Co, Fe, and especially Sr in the YSZ slab, within a 1  $\mu\text{m}$  region from the interface. Thus the formation of a distinct Sr-zirconate phase was suspected close to the interface, which is in line with the observations reported in the literature.<sup>21</sup> However, the diffusion of strontium did not seem to have significantly altered the composition of the pellet near the interface.

For a  $\text{SrFeCo}_{0.5}\text{O}_x$ -YDC cell, similar investigations showed that strontium had also diffused into the electrolyte,  $\sim 1/2 \mu\text{m}$  from the interface. Thus, the formation of an interfacial Sr-cerate phase cannot be excluded. At the same time in the cobaltate, close to the interface, a significant amount of Ce and relatively small Fe and Co were detected. However, the interfacial morphology and structure of the pellet were not altered; EDX analysis of a 10  $\mu\text{m}$  region adjacent to the interface indicated the expected stoichiometric ratios of the components of the  $\text{SrFeCo}_{0.5}\text{O}_x$  compound.

### Discussion

**Chemical diffusion coefficients.**—This work has demonstrated the usefulness of using asymptotic expressions in fitting relaxation data due to diffusion, particularly in ascertaining whether the mathematical model is fully representative of the physical phenomenon under investigation. This is especially true for the present study, since any diffusional process can be fitted to a series of exponentials regardless of the extent of irreversibility of the interface. The short-time analysis in the present study was found to be very useful in verifying the surface exchange limitation and identifying the presence of a short-time capacitive effect resulting from the exchange of gas from interfacial pockets. At the same time, the long-time response, as long as properly corrected for the surface irreversibility and leakage, gives a reliable chemical diffusion coefficient, since the concentration dependence of this parameter diminishes with vanishing concentration gradient.

The present approach validated that oxygen transport within the samples occurs by lattice diffusion, and that the overall transport rate is partially controlled by the surface exchange reaction, in the materials investigated. This is supported by the consistency of results for the compound  $\text{SrCo}_{0.5}\text{Fe}_{0.5}\text{O}_{3-\delta}$  obtained from the blocked and open cells. For example, if high-diffusivity paths were present, as claimed by Sunde et al.<sup>5</sup> in specimens of the  $\text{SrCo}_x\text{Fe}_{1-x}\text{O}_{3-\delta}$  family, then the blocked cell would give data characteristic of intragrain diffusion,<sup>5</sup> while the open cell would give results characteristic of diffusion along the high diffusivity paths, two phenomena associated with widely different diffusion rates. As discussed at length in Ref. 5, the long time data correspond to the process with the largest time constant, which in turn corresponds to transport of oxygen from the individual grains. Since the oxygen drawn in response to the potential step is provided by the specimen, the current is limited by transport of vacancies in the grain bodies and exchange at the grain surfaces. In the case of the open cell, the oxygen flux is determined by the path providing the highest diffusion rate through the specimen, as the sample itself contributes only a small fraction of the total measured flux.

As an additional evidence to the present claim, we found that the time constants for relaxation are dependent on the thickness of the pellet, whereas the time constant should depend on the grain size rather than the pellet thickness in the presence of high diffusivity paths.<sup>5</sup>

It was not possible to obtain a linear  $I$ - $V$  relationship for  $\text{SrFeCo}_{0.5}\text{O}_x$  in open cell measurements. Lower enhancement factors estimated from the slope of the  $I$ - $V$  data in the limit of zero current would suggest a higher chemical diffusion coefficient for oxygen than indicated by the blocked cell data. Similarly, the ionic conductivity of the material estimated from the chemical diffusion coefficient and enhancement factor (or nonstoichiometry) data of the blocked cell, by use of Eq. 2 and the Nernst-Einstein relationship, cannot be reconciled with much higher values measured by direct conductivity measurements of Ma et al.<sup>12</sup> A possible cause of these inconsistencies is the presence of high diffusivity paths as discussed above. Another possible explanation of the anomalous behavior of  $\text{SrFeCo}_{0.5}\text{O}_x$  is decomposition or the multiphase nature of this material as reported by Gugilla and Manthiram.<sup>20</sup> The present data with the open cell are too scarce to reach any conclusions about the behavior of  $\text{SrFeCo}_{0.5}\text{O}_x$ . In any event, the blocked cell data for  $\text{SrFeCo}_{0.5}\text{O}_x$  are consistent with the relaxation data of Ma et al.,<sup>3</sup> in view of the similarity of the chemical diffusion coefficients (with reservation discussed below) and activation energy reported in the two studies by use of two different, but related, methods.

If the surface exchange process were assumed to be reversible, the time constant for the current relaxation at large times would be expressed as  $(2L/\pi)^2/\tilde{D}_{\text{eff}}$ ,<sup>5</sup> where  $\tilde{D}_{\text{eff}}$  is the effective diffusion coefficient which would be calculated with this assumption. When compared to the true time constant indicated by Eq. 8, the error in the measured diffusion coefficient can be expressed as<sup>8</sup>

$$\frac{\tilde{D}_{\text{eff}}}{\tilde{D}} = \left( \frac{2\lambda_1}{\pi} \right)^2 \quad [16]$$

Thus, the error incurred by assuming reversibility of the surface exchange reaction can be visualized by plotting the right side of Eq. 16 as a function of  $kL/\tilde{D}$  as shown in Fig. 8. There is no error in the limit as  $kL/\tilde{D} \rightarrow \infty$ , i.e., for a reversible boundary condition. As  $kL/\tilde{D}$  becomes small, however, corresponding to increasing irreversibility of the surface, the measured diffusion coefficient becomes smaller than the true value. For the specimens used in this study, the ratio  $\tilde{D}_{\text{eff}}/\tilde{D}$  lies in the range 0.07 to 0.26 for  $\text{SrCo}_{0.5}\text{Fe}_{0.5}\text{O}_{3-\delta}$ , and 0.11 to 0.5 for  $\text{SrFeCo}_{0.5}\text{O}_x$ .

Significantly lower diffusion coefficient values reported by Nisançioğlu and Gür<sup>4</sup> may thus testify to the presence of surface irreversibilities. However, since the measurement on powdered and sintered specimens gave similar responses,<sup>5</sup> their results may have been affected by the presence of microcracks, which can easily result from thermal cycling, as indicated by the present study, especially in the presence of interfacial reactions between the specimen and the electrolyte.

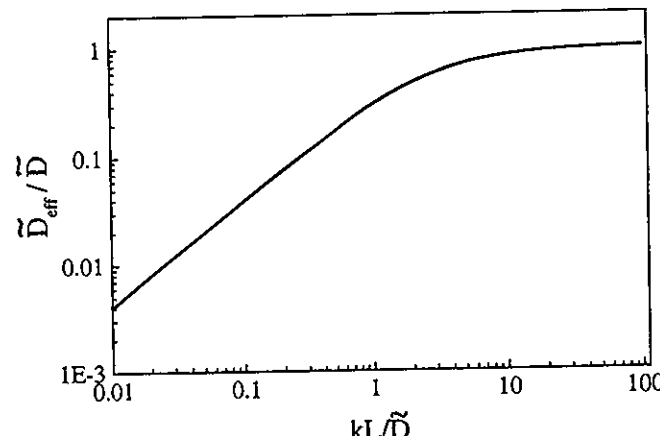


Figure 8. The effect of reaction rate limitation at the surface on the chemical diffusion coefficient estimated with the assumption of surface reversibility.

Table II. Comparison of the data for chemical diffusion and surface exchange coefficients and activation energies for different types of cobaltates and ferrates.

Material	T (°C)	$\tilde{D}$ (cm <sup>2</sup> /s)	$E_a$ (kJ/mol)	$k$ (cm/s)	Ref.
$\text{SrCo}_{0.5}\text{Fe}_{0.5}\text{O}_{3-\delta}$	800	$2.2 \cdot 10^{-6}$	$200 \pm 25$	$8.9 \cdot 10^{-6}$	This work
	900	$1.9 \cdot 10^{-5}$		$5.2 \cdot 10^{-5}$	
$\text{SrFeCo}_{0.5}\text{O}_x$	800	$9.2 \cdot 10^{-7}$	$70 \pm 35$	$2.3 \cdot 10^{-6}$	This work
	900	$2.4 \cdot 10^{-6}$		$8.3 \cdot 10^{-6}$	
$\text{SrFeCo}_{0.5}\text{O}_x$	800	$2.5 \cdot 10^{-7}$	89	—	3
	900	$8.9 \cdot 10^{-7}$		—	
$\text{La}_{0.6}\text{Sr}_{0.4}\text{FeO}_{3-\delta}$	800	$1.1 \cdot 10^{-5}$	$80 \pm 25$	$6.8 \cdot 10^{-6}$ a	6
	875	$1.9 \cdot 10^{-5}$		$1.5 \cdot 10^{-5}$ a	
$\text{La}_{0.8}\text{Sr}_{0.2}\text{CoO}_{3-\delta}$	800	$1.5 \cdot 10^{-6}$	$135 \pm 7$	—	7
	900	$7.5 \cdot 10^{-6}$		—	
$\text{La}_{0.6}\text{Sr}_{0.4}\text{Co}_{0.6}\text{Fe}_{0.4}\text{O}_{3-\delta}$	782 <sup>b</sup>	$5.6 \cdot 10^{-6}$	$95 \pm 4$ b	$1.0 \cdot 10^{-5}$ a	22
	800 <sup>b</sup>	$1 \cdot 10^{-5}$	$117 \pm 5$ c	—	
	875 <sup>c</sup>	$2.5 \cdot 10^{-5}$		—	
	882 <sup>b</sup>	$1.3 \cdot 10^{-5}$		$2.0 \cdot 10^{-5}$ a	

<sup>a</sup> Data for an oxygen partial pressure of  $\sim 10^{-1}$  bar.<sup>b</sup> Electrical conductivity relaxation measurement.<sup>c</sup> Coulometric titration relaxation measurement.

**Surface exchange coefficients.**—As mentioned earlier in the paper, the  $k$  values obtained from blocked cells with gold ring spacers can only be considered as representative surface exchange coefficients. Furthermore, no platinum deposition, which would have influenced  $k$ , was detectable from EDX investigation of the surface of the specimen, even if such an analysis cannot be regarded as conclusive. The  $k$  values obtained from blocked cells without spacers should be viewed with care in the light of the SEM interfacial examinations. However, the chemical diffusion coefficients obtained from such cells are still valid, since the bulk transport properties should not be affected by the variations in the surface properties, as long as the data analysis takes into account such surface limitations.

**Comparison with literature data.**—Since data related to the same materials are scarce, we include data for other types of Sr-doped cobaltates and ferrates in the comparison given Table II. Furthermore, since the surface exchange coefficients depend strongly on the oxygen partial pressure,<sup>6,22</sup> values similar to the conditions used in the present study were chosen for a consistent comparison. The partial pressure corresponding to a  $-20$  mV reduction step is  $\sim 0.17$  bar at  $800^\circ\text{C}$  and  $\sim 0.16$  bar at  $900^\circ\text{C}$ .

As mentioned above for  $\text{SrFeCo}_{0.5}\text{O}_x$ , the chemical diffusion coefficients obtained in this study agree well with those reported in the literature,<sup>3</sup> if one takes into account the fact that the model considered in Ref. 3 for the data analysis assumes reversible surfaces. The values calculated for the chemical diffusion coefficient with this assumption is expected to be lower than the actual value as discussed above with reference to Fig. 8. For the other compounds, the agreement is good with the results reported in this paper within the limits of scatter.

### Conclusions

Potentiostatic relaxation data obtained from a blocked electrochemical cell for the compounds  $\text{SrCo}_{0.5}\text{Fe}_{0.5}\text{O}_{3-\delta}$  and  $\text{SrFeCo}_{0.5}\text{O}_x$  were analyzed by using a one-dimensional diffusion model for oxygen including surface exchange limitations. The methodology developed involves curve-fitting the experimental relaxation data to asymptotic forms of the transient flux expression valid at short and long times, and this approach gives the possibility for various consistency checks to ascertain that the theoretical model is satisfied. Chemical diffusion coefficients could be obtained, despite the formation of interfacial phases due to the reaction between the specimen and the electrolyte. By avoiding interfacial reactions with the use of a gold ring spacer between the specimen and the electrolyte, reliable data were measured for the surface exchange coefficient.

The comparison with data obtained from steady-state measurements performed on an oxygen-permeation cell showed a good agreement for the first compound. This further confirmed the validity of the electrochemical approach and the assumption of one-dimensional lattice diffusion in data analysis.

### Acknowledgments

K.N. was a visiting professor at LPI, EPFL, during part of this work. This work was supported by the Federal Office of Energy (CH), the Priority Program for Materials (CH), Norsk Hydro a.s. (N), Statoil a.s. (N), and the Research Council of Norway.

*École Polytechnique Fédérale de Lausanne assisted in meeting the publication costs of this article.*

### References

1. A. Belzner, T. M. Gür, and R. A. Huggins, *Solid State Ionics*, 40/41, 535 (1990).
2. A. Belzner, T. M. Gür, and R. A. Huggins, *Solid State Ionics*, 57, 327 (1992).
3. B. Ma, U. Balachandran, J.-H. Park, and C. U. Segre, *Solid State Ionics*, 83, 65 (1996).
4. K. Nisancioglu and T. M. Gür, *Solid State Ionics*, 72, 199 (1994).
5. S. Sunde, K. Nisancioglu, and T. M. Gür, *J. Electrochem. Soc.*, 143, 3497 (1996).
6. J. E. ten Elshof, M. H. R. Lankhorst, and J. M. Bouwmeester, *J. Electrochem. Soc.*, 144, 1060 (1997).
7. M. H. R. Lankhorst and J. M. Bouwmeester, *J. Electrochem. Soc.*, 144, 1261 (1997).
8. F. Viani, V. Dovi, and F. Gesmundo, *Oxid. Met.*, 21, 309 (1984).
9. F. Gesmundo, F. Viani, and V. Dovi, *Oxid. Met.*, 23, 141 (1985).
10. J. A. Kilner, in *The 2nd International Symposium on Ionic and Mixed Conducting Ceramics*, T. A. Ramanarayanan, W. L. Worell, and H. L. Tuller, Editors, PV 94-12, p. 174, The Electrochemical Society Proceedings Series, Pennington, NJ (1994).
11. Y. Teraoka, H.-M. Zhang, S. Furukawa, and N. Yamazoe, *Chem. Lett.*, p. 1743, The Chemical Society of Japan (1985).
12. B. Ma, U. Balachandran, J.-H. Park, and C. U. Segre, *J. Electrochem. Soc.*, 143, 1736 (1996).
13. J. Vanherle, T. Horito, T. Kawada, N. Sakai, H. Yokokawa, and M. Dokiya, *Solid State Ionics*, 86-88, 1255 (1996).
14. H. Rickett, *Electrochemistry of Solids*, Springer-Verlag, Berlin (1982).
15. W. Weppner and R. A. Huggins, *J. Electrochem. Soc.*, 124, 1569 (1977).
16. J. Crank, *The Mathematics of Diffusion*, 2nd ed., Oxford University Press, London (1975).
17. H. S. Carslaw and J. C. Jaeger, *Conduction of Heat in Solids*, 2nd ed., Oxford University Press, Oxford (1959).
18. W. Weppner and R. A. Huggins, in *Annual Review of Materials Science*, Vol. 8, R. A. Huggins, Editor, p. 269, Annual Reviews, Inc., Palo Alto, CA (1978).
19. M. Mugnaioli, T. Lindquist, U. R. Hansen, and O. Mugnaioli, *J. Electrochem. Soc.*, 141, 2122 (1994).
20. S. Guggilla and A. Manthiram, *J. Electrochem. Soc.*, 144, L120 (1997).
21. G. Stochniol, E. Syskakis, and A. Naoumidis, in *SOFC Materials, Process Engineering and Electrochemistry*, Proceedings of 5th IEA Workshop, March 2-4, 1993, Forschungszentrum Jülich, Germany (1993).
22. J. E. ten Elshof, M. H. R. Lankhorst, and H. J. M. Bouwmeester, *Solid State Ionics*, 99, 15 (1997).